Comparison of Sputter-deposited Single and Multilayer Electrolytes based on Gadolinia-doped Ceria and Yttria-stabilized Zirconia for Solid Oxide Fuel Cells

Andrey A. Solovyev[1,], Sergey V. Rabotkin[1], Kairat A. Kuterbekov[2], Temirgaly A. Koketay[2], Serik A. Nurkenov[2], Serikzhan Opakhai[2], Anna V. Shipilova[1], Igor V. Ionov[1], Galina M. Eliseeva[3]*

[1] Laboratory of Applied Electronics, Institute of High Current Electronics, Siberian Branch of the Russian Academy of Sciences, Tomsk, Russia
[2] Faculty of Physics and Technical Sciences, Gumilev Eurasian National University, Nur-Sultan (Astana), Kazakhstan
[3] Laboratory of spectroscopy of defective structures, Institute of Solid State Physics Russian Academy of Sciences, Chernogolovka, Russia
[*]E-mail: andrewsol@mail.ru

Single and multilayer electrolytes for anode-supported solid-oxide fuel cells (SOFCs) have been prepared by reactive magnetron sputtering and their electrochemical properties have been investigated. Electrolyte layers based on gadolinia-doped ceria (GDC) and yttria-stabilized zirconia (YSZ) were formed on NiO/YSZ substrates. The cells with single (YSZ), double (YSZ-GDC) and triple-layer (GDC-YSZ-GDC) electrolytes were tested, with the thickness of each electrolyte layer from 1 to 5 µm. The maximum cell performances of 460 and 2580 mW/cm^2 were obtained for the SOFC with triple-layer electrolyte at the operating temperature of 600°C and 800°C respectively. The thickness of each electrolyte layer was about 3, 1 and 1 µm respectively. The advantages of multilayer over single-layer electrolytes are discussed.

1. INTRODUCTION

Solid oxide fuel cells (SOFCs) are environmentally friendly energy sources with high fuel efficiency and fuel flexibility. Numerous studies are currently being conducted that aim at reducing the operating temperature of SOFC to below 800°C by reducing the thickness of the electrolyte and using electrolyte materials with a higher conductivity than that of the state-of-the-art yttria-stabilized zirconia (YSZ) [1–3].

There are several methods for thin electrolyte film formation, such as sol-gel [4], colloidal [5], electrophoretic deposition [6] and methods of physical vapor deposition [7, 8]. However, the best method should be suitable for the mass market. By using the magnetron sputtering method, uniform thin films can be obtained on the large area substrates at a reasonably low temperature (<600°C) [9]. Sønderby et al. [10] demonstrated the possibility of magnetron deposition of the YSZ electrolytes of up to 3 µm thick on the anodes, with an area of 13×13 cm^2.

In our previous work, we demonstrated the possibility of 4–6 µm thick single-layer yttria-stabilized zirconia (YSZ) and gadolinia-doped ceria (GDC) electrolyte layers formation by reactive magnetron sputtering [11, 12]. The maximum output performance of 2 mm diameter anode-supported cells with single-layer YSZ and GDC electrolytes was 1.2 W/cm^2 at 800°C and 1.07 W/cm^2 at 750°C respectively. At an operating temperature below 650–700°C, the use of doped ceria as an electrolyte increases the efficiency of SOFC, because it has a higher ionic conductivity than YSZ. In addition, doped ceria shows higher compatibility with cathodes than YSZ. However, the use of an electrolyte based on cerium oxide leads to a reduction in open-circuit voltage (OCV) – due to the appearance of electronic conductivity in it in a reducing atmosphere. Considering the proven reliability of YSZ electrolyte in long-term tests [13], its use in SOFC appears to be the most logical choice. Therefore, the use of a thin layer of YSZ electrolyte, applied between two layers of GDC, in order to block the electronic conductivity of the GDC electrolyte [14–16], is a promising approach.

Suzuki *et al.* [14] prepared multilayered GDC-ScSZ-GDC electrolyte on an anode tube by using multiple dip coating and a co-firing technique. The thickness of each electrolyte layer was approximately 3,3, and 12 µm, respectively. The cells showed an open-circuit voltage of over 1 V and a power density of 0.35 W/cm^2 at 0.7 V at the operating temperature of 650°C.

Horita *et al.* [15] used a doctor blade method and a co-fire process to fabricate thick GDC-YSZ-GDC (70/7/70 µm) electrolyte. The main problems with this approach were the different shrinkage behavior of the ceria and zirconia green films and the unsatisfactory mechanical strength of the composite film. In addition, high-temperature sintering resulted in an inevitable chemical reaction between GDC and YSZ.

By using 100 nm thick YSZ layer, Noh *et al.* [16] obtained the most impressive results for GDC-YSZ-GDC tri-layers. Electrolyte with layers thickness of 1/0.1/1 µm respectively was deposited on NiO/YSZ support by using pulsed laser deposition. The thin-film solid oxide fuel cell demonstrated a high open-circuit voltage of 1.05 V and a peak power density of about 2.1 W/cm^2 at 650°C.

In the current study, a triple-layer GDC-YSZ-GDC electrolyte was deposited on NiO/YSZ anodes by reactive magnetron sputtering. The performance of the cell was investigated and compared to that of the cells with a single-layer (YSZ) and double-layer (YSZ-GDC) electrolyte. The effect of the number and thickness of electrolyte layers on the characteristics of the SOFC was investigated.

2. EXPERIMENTAL

Electrolyte layers were deposited on the commercial NiO/10ScCeSZ anodes (KCERACELL CO., Korea) by means of reactive magnetron sputtering. The substrates were mounted on a rotating drum with a rotation speed of 1.5 rpm and, due to the rotation, the substrates were facing the sputtered

targets only part of the time. When the substrates were facing the targets directly, the distance between them was 10 cm. Two targets (30×10 cm^2) were positioned on the sidewalls of the vacuum chamber – metallic Zr-Y (85:15 at.%) and Ce-Gd (90:10 at.%). Before the deposition, the substrates with a diameter of 20 mm were ultrasonically cleaned, after which the substrates were cleaned in a vacuum chamber by means of an ion source with closed electron drift. The ion treatment lasted 10 minutes, at a discharge voltage of 2 kV and a discharge current of 100 mA. The residual pressure in the vacuum chamber was $1.0 \cdot 10^{-2}$ Pa, while working pressure was 0.2 Pa and the argon flow rate was 90 sccm. The oxygen flow rate during YSZ and GDC deposition was 37.5 and 13.5 sccm respectively. The deposition was performed with a constant average discharge power of 4 kW for Zr-Y target and 3 kW for Ce-Gd target. All depositions were made at a substrate temperature of 350°C. After the electrolyte deposition, the samples were post-annealed at 1200°C for 1 h to improve the crystallinity of the electrolyte.

La$_{0.6}$Sr$_{0.4}$CoO$_3$ (LSC) cathode (KCERACELL CO., Korea) with an active area of 10×10 mm^2 was screen printed onto the electrolyte and fired *in situ* during the cell test start-up. Electrochemical investigations were performed in the temperature interval of 600–800 °C at the constant supply of dry hydrogen (120 ml/min) to the anode and the air (350 ml/min) to the cathode. Ag mesh and Pt wires were used for current collecting from the anode and cathode. The electrochemical impedance spectra (EIS) and current-voltage (I-V) curves were obtained at each temperature. Z-500P impedance meter and P-150S potentiostat (Elins, Russia) were used to obtain EIS and I-V curves. The impedance was measured in the frequency range of 0.1–$5 \cdot 10^5$ Hz and the AC signal amplitude of 5 mV under open-circuit conditions.

A scanning electron microscope (SEM) LEO Supra 50VP was used to study the microstructure of fabricated cells. Some SEM images were obtained by using a Dual Beam VERSA 3D HighVac (FEI) setup.

3. RESULTS AND DISCUSSION

3.1. Cells with single-layer YSZ electrolyte

In order to form gas-tight electrolytes with a thickness of hundreds of nanometers or a few microns, the surface of the anodes must be very smooth, have a small porosity and a minimum pore size (from few hundreds to few tens of nanometers). Fig. 1a shows a cross-sectional SEM image of anode substrate in its original (oxidized) form. The image was obtained in mode with secondary electrons (SE). A porous anode with a thickness of 500 μm has an anode functional layer (AFL) with a thickness of 10 μm. AFL has a much denser structure compared to that of the main anode layer. However, as can be seen in Fig. 1b, after reduction in hydrogen, the AFL becomes sufficiently porous, with a pore size of about 1–1.5 μm.
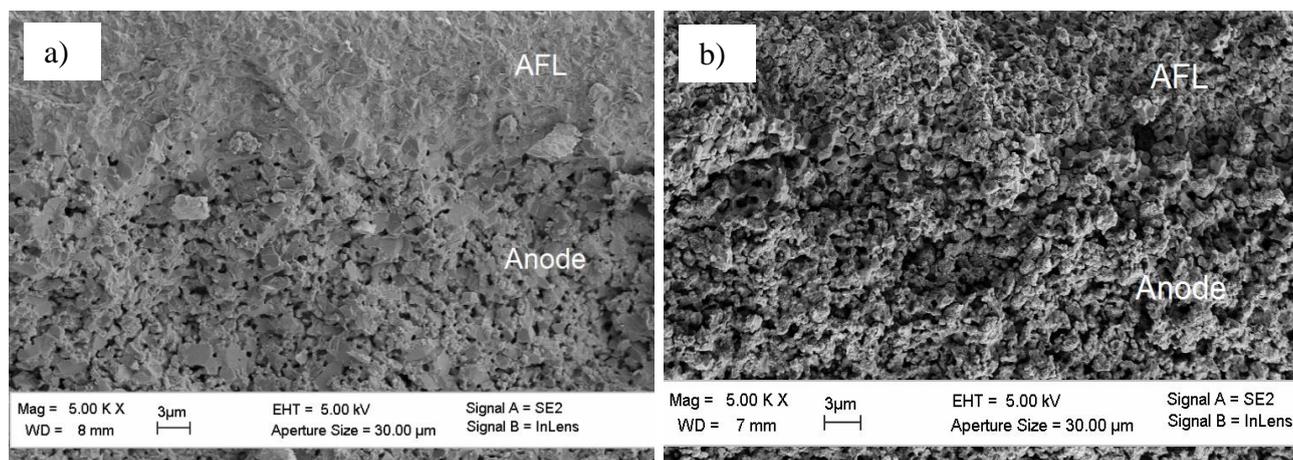
Figure 1. Cross-sectional SEM micrographs of the anode substrates: (a) in an oxidized state; (b) after reduction in hydrogen (secondary electrons mode)

In order to evaluate the minimum thickness of the electrolyte for this anode, which reliably ensures its gas impermeability, cells with a single-layer YSZ electrolyte, with a thickness of 3.2 and 5.3 μm were manufactured. The OCV and power density values of these cells, measured at different temperatures, are shown in Table 1. An OCV of approximately 1.08–1.13 V was obtained over the entire temperature range for both cells, which confirms the electrolyte thickness of 3 μm being sufficient for its gas tightness. The highest values of power density over the entire temperature range were shown by a cell with a thinner electrolyte. With a decrease in the thickness of the electrolyte from 5.3 to 3.2 μm, the power density increased from 1857 to 2300 mW/cm^2 at a temperature of 800°C and from 115 to 235 mW/cm^2 at 600°C. This can evidently be ascribed to the lower ohmic resistance of the cell with the thinner electrolyte.

Table 1. OCV and peak power density (P_{max}) values of the SOFCs with the single and multilayer electrolyte at different working temperatures

Electrolyte (thickness)	Parameters	Working temperature				
		800°C	750°C	700°C	650°C	600°C
YSZ (3.2 μm)	OCV, mV	1080	1130	1133	1121	1100
	P_{max}, mW/cm^2	2300	1590	950	480	235
YSZ (5.3 μm)	OCV, mV	1098	1123	1127	1121	1097
	P_{max}, mW/cm^2	1857	1088	589	280	115
YSZ–GDC (3.2/1μm)	OCV, mV	1097	1104	1113	1113	1105
	P_{max}, mW/cm^2	2510	1850	1331	804	390
YSZ–GDC (5.3/1.8 μm)	OCV, mV	1122	1160	1170	1175	1180
	P_{max}, mW/cm^2	2400	1915	1220	633	290
GDC–YSZ–GDC	OCV, mV	878	901	905	896	884

(3/0.5/1 µm)	P_{max}, mW/cm^2	2000	1790	1368	754	353
GDC–YSZ–GDC (3/1/1 µm)	OCV, mV	1060	1070	1080	1081	1076
	P_{max}, mW/cm^2	2580	2100	1506	911	460

3.2. Cells with double-layer YSZ–GDC electrolyte

It is known that a diffusion barrier layer is needed between the LSC cathode and the YSZ electrolyte, because Sr and La from the cathode react with Zr from the electrolyte during operation [17]. A double-layer electrolyte takes advantage of both layers. The advantages of YSZ are excellent stability and low electronic conductivity, while the advantages of GDC are high ionic conductivity and low reactivity with a cathode. Therefore, cells with a double-layer YSZ-GDC electrolyte were fabricated and tested, in order to determine the effect of the GDC barrier layer on the characteristics of the cells. Two cells were fabricated and compared. In one cell, the layers of the YSZ-GDC electrolyte were 3.2 and 1 µm thick respectively. In another cell, these layers had a thickness of 5.3 and 2 µm.

Fig. 2a shows a cross-sectional SEM image of anode substrate with deposited YSZ-GDC (3.2/1µm) electrolyte (after annealing in air at 1200°C).
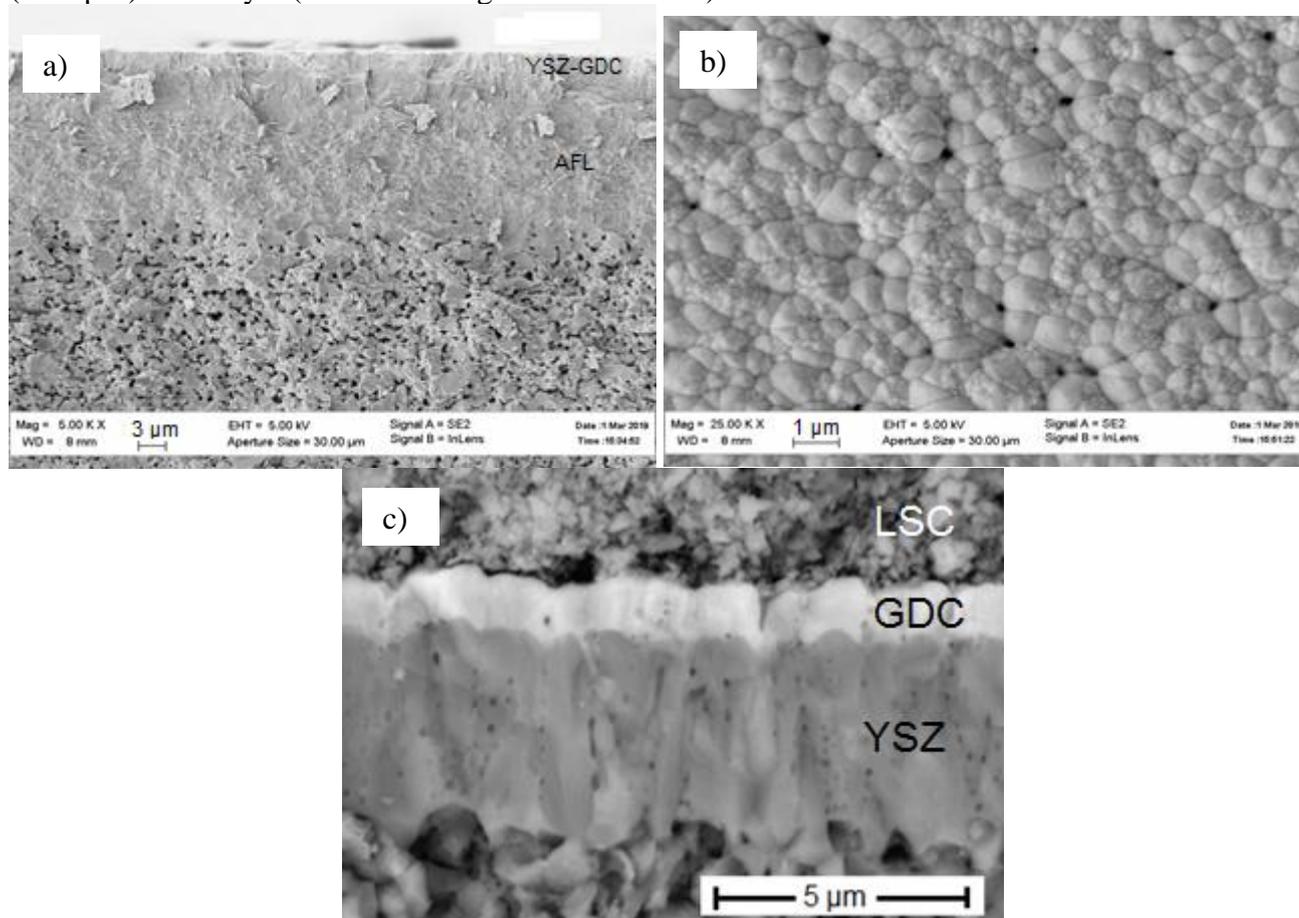
Figure 2. Cross-sectional SEM micrograph (SE mode) of the double-layer YSZ-GDC electrolyte deposited on anode support in an oxidized state (a); the surface of the GDC barrier layer (b); the enlarged image of YSZ-GDC electrolyte after testing (backscattered electron image) (c).

As it can be seen, the double-layer electrolyte has good adhesion to the anode and the boundary between them is hardly distinguishable. The surface of the GDC layer (Fig. 2b) has a granular structure, with densely packed grains ranging in size from 200 nm to 1.5 µm. In Fig. 2c, backscattered electrons were used for phase contrast and the GDC is clearly defined as the brighter layer on the top of the YSZ electrolyte. This image was obtained after cell testing and, therefore, the anode is in a reduced state. It is possible to observe good adhesion between the YSZ and GDC layers and satisfactory contact of the latter with the anode – even after its reduction and pore formation.

As shown in Fig. 2c, the cathode layer, on the other hand does not adhere well to the electrolyte, due to the low sintering temperature. Despite the fact that the test temperature did not exceed 800°C and that the total thickness of the electrolyte increased, cells with a double-layer electrolyte demonstrated a high performance – even better than that of cells with a single-layer electrolyte (Table 1). In both cases (with a 3.2 and 5.3 µm-thick YSZ electrolyte), the deposition of a GDC barrier layer resulted in an increase in the power density of the cell, while maintaining a high level of OCV. The deposition of a 1 µm thick GDC layer on 3.2 µm thick YSZ electrolyte resulted in an increase in peak power density from 2300 to 2510 mW/cm^2 at a temperature of 800°C and from 235 to 390 mW/cm^2 at a temperature of 600°C, in comparison to a cell with a single-layer electrolyte. It is worth noting that the greatest increase in power was observed at lower temperatures. Mukai *et al.* [18] obtained close values of power density (400 mW/cm^2 at 600°C) for an anode-supported cell with an YSZ-GDC (3/5 µm) double-layer electrolyte and a $Gd_{0.5}Sr_{0.5}CoO_3$ cathode, which were deposited by pulsed laser deposition.

The power enhancement in the use of a double-layer electrolyte can probably be ascribed to the fact that cathodic interface resistance is reduced after GDC layer deposition. Park *et al.* [19] and Fan *et al.* [20] showed that the deposition of thin films of GDC or YDC (yttria-doped ceria) on the YSZ electrolyte leads to the reduction in cathode/interfacial activation energy and an increase in exchange current density. Kim *et al.* [21] found that activation energy for oxygen incorporation was about 0.38 eV for YSZ and only 0.07 eV for YDC. This points to a superior performance of the LSC cathode contact with the GDC electrolyte, compared to that of the YSZ electrolyte.

3.3. Cells with triple-layer GDC-YSZ–GDC electrolyte

To reduce the ohmic resistance of the electrolyte, it is necessary to reduce the thickness of the YSZ layer, since YSZ has a higher resistance than GDC. In a triple-layer electrolyte, the YSZ layer must be not only thin, but also continuous to block the electronic conductivity of the GDC. The bottom layer of the GDC must be thick enough to cover defects on the surface of the anode, which may disrupt the integrity of the YSZ layer. Based on these considerations, two cells with a triple-layer GDC-YSZ-GDC electrolytes were manufactured in which the layer thickness was 3/0.5/1 µm and 3/1/1 µm.

Fig. 3 shows a cross-sectional SEM image of the cell with GDC-YSZ-GDC (3/1/1 µm) electrolyte, after testing. The electrolyte has a dense structure in which the three layers are well integrated with one another.

As reflected in Table 1, the cell with a triple-layer electrolyte (3/0.5/1 µm), in which the YSZ layer has a thickness of 0.5 µm, has low OCV values (0.87–0.9 V) over the entire temperature range. This means that the thickness of the YSZ layer is not enough to ensure its continuity. However, a cell with a three-layer electrolyte, which has a layer thickness of 3/1/1 µm, shows stable OCV values above 1.06 V. This result indicates the effectiveness of the YSZ layer to block the leakage current that causes the drop of the OCV.
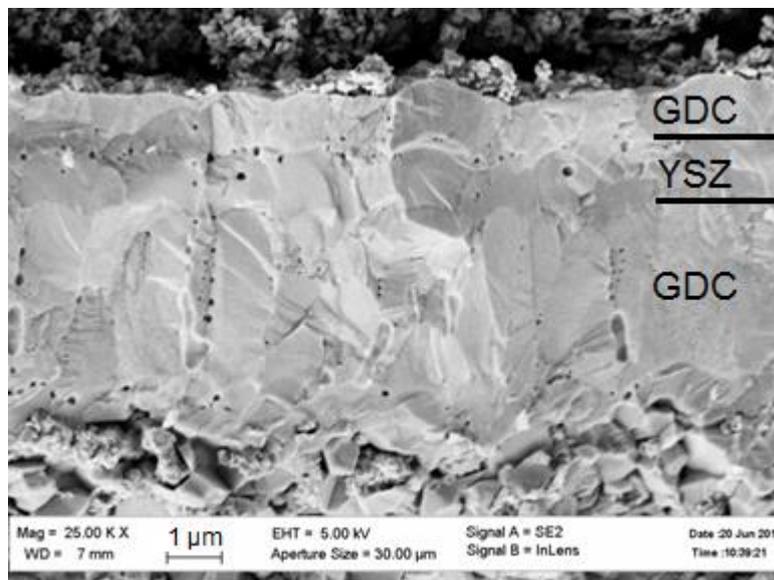
Figure 3. Cross-sectional SEM image of a single cell with a triple-layer GDC-YSZ-GDC (3/1/1 µm) electrolyte

Fig. 4a shows the current-voltage (I-V) and current-power (I-P) characteristics of a single cell with a triple-layer GDC-YSZ-GDC (3/1/1 µm) electrolyte. The peak power density ranges between 460 mW/cm^2 at 600°C and 2580 mW/cm^2 at 800°C. This cell shows the highest efficiency of all the cells shown in Table 1.
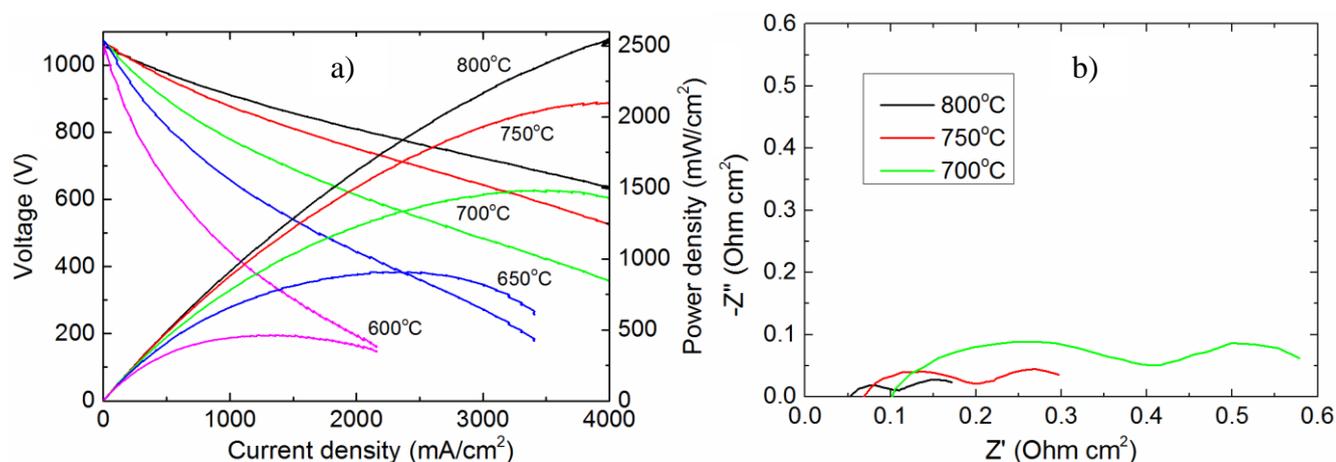
Figure 4. I-V and I-P curves measured in the 600–800°C range for the single cell with a triple-layer GDC-YSZ-GDC (3/1/1 µm) electrolyte (a) and impedance spectra of this cell at different operating temperatures (b).

The impedance spectra of the single cell with a triple-layer electrolyte measured under open-circuit conditions between 700 and 800°C are given in Fig. 4b. By decreasing the operation temperature, both ohmic and polarization resistance increased because of the reduction of material conductivity and reaction kinetics. When the temperature was lowered from 800°C (0.053 Ohm·cm^2) to 700°C (0.102 Ohm cm^2), the ohmic resistance increased by two times. The polarization resistance increased nearly by 3.5 times, from 0.15 Ohm·cm^2 at 800°C to 0.52 Ohm·cm^2 at 700°C. The lower the temperature, the greater the contribution the polarization resistance of the cathode makes to the overall polarization resistance, because the latter is usually shown as very low electrochemical activity at low temperatures.

Table 2 summarizes the reported power densities of the anode-supported SOFCs with thin-film double-layer YSZ-GDC and triple-layer GDC-YSZ-GDC electrolyte fabricated with different techniques. In some cases, the magnetron sputtered electrolytes demonstrated a far better performance than the electrolytes made by screen-printing, dip coating, or even pulsed laser deposition [23, 14, 18, 22]. Although it is possible to achieve more than 2 W/cm^2 power densities at 650°C with the use of a very thin electrolyte layer or thin nano and gradient-structured cathodes [16, 25], the magnetron sputtered electrolytes allow obtaining very high performance.

Table 2. Comparison of the characteristics of the anode-supported SOFCs with thin-film double-layer YSZ-GDC and triple-layer GDC-YSZ-GDC electrolyte

Electrolyte	Layers thickness	Fabrication method	Cathode	Performance	Ref.
YSZ-GDC	3/5 μm	Pulsed laser deposition	GSCO	P$_{max}$ = 400, 450 and 500 mW/cm^2 at 600, 650 and 700°C	[18]
YSZ-GDC	0.33/6 μm	Pulsed laser deposition	LSC/GDC	P$_{max}$ = 188, 430 and 587 mW/cm^2 at 650, 700 and 750°C	[22]
YSZ-GDC	5/5 μm	Screen printing	LSCF/GDC	P$_{max}$ = 1400 mW/cm^2 at 750°C. Fabrication of large cells (10 cm × 10 cm^2) is demonstrated.	[23]
YSZ-GDC	6/0.15 μm	Screen printing (YSZ) and aerosol-assisted chemical vapor deposition (GDC)	LSC	P$_{max}$ = 850 mW/cm^2 at 650°C	[24]
YSZ-GDC	6/0.5μm	Spin coating	Thin nanostructured LSCF	P$_{max}$ = 2140 and 1290 W/cm^2 at 650 and 550°C	[25]
YSZ-GDC	3.2/1 μm	Magnetron sputtering	LSC	P$_{max}$ = 2510 and 390 W/cm^2 at 800 and 600°C	This work
GDC-ScSZ-GDC	3/3/12 μm	Dip coating	LSCF	P$_{max}$ = 400 mW/cm^2 at 650°C	[14]

Electrolyte	Layers thickness	Fabrication method	Cathode	Performance	Ref.
GDC-YSZ-GDC	1/0.1/1 µm	Pulsed laser deposition	Gradient-structured LSC/GDC	P_{max} = 2100 mW/cm^2 at 650°C	[16]
GDC-YSZ-GDC	3/1/1 µm	Magnetron sputtering	LSC	P_{max} = 2580 and 911 W/cm^2 at 800 and 650°C	This work

4. CONCLUSIONS

The paper compares the characteristics of SOFC with single (YSZ), double (YSZ-GDC) and triple-layer (GDC-YSZ-GDC) electrolytes of different thickness deposited by reactive magnetron sputtering. Cells with a double-layer YSZ-GDC electrolyte show better performance than cells with a single-layer YSZ electrolyte, because the LSC cathode demonstrates a superior performance in contact with GDC than with the YSZ, which leads to reducing the cathodic interface resistance in the first case. The formation of a triple-layer (GDC-YSZ-GDC) allows for a further increase in the SOFC power in the temperature range of 600–800°C, particularly at lower temperatures. This is because the bottom GDC layer makes it possible to reduce the thickness of the YSZ layer significantly. The maximum power density of the cell with triple-layer electrolyte was 460, 911, 1506, 2100 and 2580 mW/cm^2 at 600, 650, 700, 750 and 800°C operating temperature respectively. It should be noted that the long-term stability and resistance of such electrolytes to redox tests require additional studies.

Using pulsed laser deposition, the possibility of producing thinner electrolytes on anodes with a more perfect surface has repeatedly been demonstrated. However, unlike pulsed laser deposition, magnetron sputtering has the significant advantage of scalability on large area substrates.

References

1. S.M. Majhi, S.K. Behura, S. Bhattacharjee, B.P. Singh, T.K. Chongdar, N.M. Gokhale and L. Besra, *Int. J. Hydrog. Energy*, 36 (2011) 14930.
2. A. Tarancón, *Energies*, 2 (2009) 1130.
3. E.G. Kalinina, N.M. Bogdanovich, D.I. Bronin, E.Y. Pikalova and A.A. Pankratov, *Russ. J. Appl. Chem.*, 92(2) (2019) 191.
4. K. Lee, J. Kang, S. Jin, S. Lee and J. Bae, *Int. J. Hydrog. Energy*, 42(9) (2017) 6220.
5. J.S. Ahn, M.A. Camaratta, D. Pergolesi, K.T. Lee, H. Yoon, B.W. Lee, D.W. Jung, E. Traversa, and E.D. Wachsman, *J. Electrochem. Soc.*, 157(3) (2010) B376.
6. E. Kalinina, E. Pikalova, A. Kolchugin, N. Pikalova and A. Farlenkov, *Materials*, 12(16) (2019) 2545.

7. G. Laukaitis and J. Dudonis, *J. Alloys Compd.*, 459 (2008) 320.
8. N. Pryds, K. Rodrigo, S. Linderoth and J. Schou, *Appl. Surf. Sci.*, 255 (2009) 5232.
9. H. Hidalgo, A. ‑ L. Thomann, T. Lecas, J. Vulliet, K. Wittmann ‑ Teneze, D. Damiani, E. Millon and P. Brault, *Fuel Cells*, 13(2) (2013) 279.
10. S. Sønderby, B.H. Christensen, K.P. Almtoft, L.P. Nielsen, P. Eklund, *Surf. Coat. Tech.*, 281 (2015) 150.
11. I.V. Ionov, A.A. Solovyev, A.V. Shipilova, A.M. Lebedynskiy, E.A. Smolyanskiy, A.L. Lauk and V.A. Semenov, *Jpn. J. Appl. Phys.*, 57 (2018) 01AF07.
12. A.A. Solovyev, S.V. Rabotkin, A.V. Shipilova and I.V. Ionov, *Int. J. Electrochem. Sci.*, 14(1) (2019) 575.
13. L. Blum, W.A. Meulenberg, H. Nabielek and R. Steinberger-Wilckens, Worldwide SOFC technology overview and benchmark, *Int. J. Appl. Ceram. Technol.*, 2 (2005) 482.
14. T. Suzuki, Z. Hasan, Y. Funahashi, T. Yamaguchi, Y. Fujishiro and M. Awano, *Electrochem. Solid-State Lett.*, 11(6) (2008) B87.
15. T. Horita, N. Sakai, H. Yokokawa, M. Dokiya, T. Kawada, J. van Herle and K. Sasaki, *J. Electroceramics*, 1(2) (1997) 155.
16. H.S. Noh, J. Hong, H. Kim, K.J. Yoon, J.H. Lee, B.K. Kim and J.W. Son*, J. Ceram. Soc. Jpn.*, 123(4) (2015) 263.
17. G.C. Kostogloudis, G. Tsiniarakis and C. Ftikos, *Solid State Ion.*, 135 (2000) 529.
18. T. Mukai, S. Tsukui, K. Yoshida, S. Yamaguchi, R. Hatayama, M. Adachi, H. Ishibashi, Y. Kakehi, K. Satoh, T. Kusaka and K.C. Goretta, *J. Fuel Cell Sci. Technol.*, 10 (2013) 61006.
19. T. Park, Y.H. Lee, G.Y. Cho, S. Ji, J. Park, I. Chang, and S.W. Cha, *Thin Solid Films*, 584 (2015) 120.
20. Z. Fan, J. An, A. Iancu and F.B. Prinz, *J. Power Sources*, 218 (2012) 187.
21. Y.B. Kim, J.H. Shim, T.M. Gür and F.B. Prinz, *J. Electrochem. Soc.*, 158 (2011) B1453.
22. S. Cho, Y.N. Kim, J.H. Kim, A. Manthiram and H. Wang, *Electrochim. Acta*, 56 (2011) 5472.
23. S. Lee, S. Lee, H. Kim, S.M. Choi, H. An, M.Y. Park, J. Shin, J.H. Park, J. Ahn, D. Kim, H. Ji, H. Kim, J. Son, J. Lee, B. Kim, H. Lee, J. Hong, D. Shin and K.J. Yoon, *J. Mater. Chem. A*, 6 (2018) 15083.
24. M.V.F. Schlupp, A. Kurlov, J. Hwang, Z. Yáng, M. Döbeli, J. Martynczuk, M. Prestat, J.W. Son, and L.J. Gauckler, *Fuel Cells*, 13(5) (2013) 658.
25. I. Jang, S. Kim, C. Kim, H. Lee, H. Yoon, T. Song, and U. Paik, *J. Power Sources*, 435 (2019) 226776.